Preprints of the 2012 20th Mediterranean Conference on Control & Automation (MED), Barcelona, Spain, July 3-6, 2012

Cardiovascular Model with Human Elastance Function and Valve Dynamics

Adrian Korodi, Alexandru Codrean, Angela Timofte and Toma-Leonida Dragomir, *Member, IEEE*

***Abstract*— The cardiovascular system with its nervous control has been the focus of several mathematical modeling studies and numerous experimental investigations in the past. The purpose of the paper is to establish, by improving the existing models, an appropriate model of the cardiovascular system with its nervous control adapted to human characteristics. The research starts from a well-known model from the literature. Improvements are done in the ventricle compartments, considering the dynamics of the four heart valves and using a model for the elastance function based on human experimental data. Following correlation and calibration procedures the resulted model reveals for a normal scenario a behavior closer to reality.**

I. Introduction

THE cardiovascular diseases are widely present in all communities. The doctors are encountering problems in the diagnosis phase. As consequence, various researches and projects (e.g. Virtual Physiological Human European Project) are trying to model the human cardiovascular system (CVS) in order to provide an alternative tool to be used in the analysis and diagnosis phase of the CVS diseases. Having an adequate computational model of the CVS, the next steps would be to design patient specific algorithms, respectively to implement parameter and signal estimation techniques in order to provide the necessary information to doctors for an accurate diagnosis.

An essential attribute of a proper CVS model is the nervous control. Although there are some studies which analyze CVS models without including the nervous control (e.g. [1], [2], [7]), most studies include some form of models for the nervous control mechanisms in order to be able to determine a closed-loop response of the system (e.g. [5], [6], [19], [20], [21], [22], [23]). In [3] the authors provide a general view of the complexity of CVS that illustrates several nervous control loops in the CVS: the baroreflex mechanism, the vestibular sympathetic reflex, local-cardiac reflex and the cardiopulmonary reflex. The baroreflex mechanism is considered to be the most significant.

A. Korodi is with "Politehnica" University of Timisoara, Romania, (phone: +40-256-403355; e-mail: adrian.korodi@aut.upt.ro). His work was supported by the strategic grant POSDRU 21/1.5/G/13798, inside POSDRU Romania 2007-2013, co-financed by the European Social Fund – Investing in People.

A. Codrean is with "Politehnica" University of Timisoara, Romania, (e-mail: alexandru.codrean@aut.upt.ro).

A. Timofte is with "Politehnica" University of Timisoara, Romania, (e-mail: timofte_angela@yahoo.com).

T. L. Dragomir, Member IEEE, is with "Politehnica" University of Timisoara, Romania, (e-mail: tldragomir@yahoo.com).

Paper [4] presents a detailed study of the CVS models found in the literature. The following actions governed the analysis: the improvement of rather incomplete models (i.e. models which do not capture all the relevant dynamic behavior from a physiological or pathological point of view), model classification according to the degree of complexity, establishment of the most suitable models for further developments. The result of the study was that various models were difficult to implement (model reproducibility issues), some were at sub-cellular level or too complex (too many non-relevant parameters and blocks), some models presented non-appropriate results, some omitted various essential aspects of the CVS system and its nervous control, some models were established strictly for certain scenarios without the possibility to be used for example in the diagnosis of a myocardial infarction or an hemorrhage, etc.

Considering these aspects, the chosen most appropriate models for the purpose of the current research were presented in [5] and [6]. Each of the models considers only the baroreflex mechanism for nervous control. The authors believe that the model from [5] provides a complete representation of the baroreflex mechanism and it is the most appropriate as a starting point for further developments. Parts of model from [6] are modeled considering experimental characteristics taken over from humans, selected as being necessary to be introduced in a future model. Also, authors considered that certain parts from both models had to be replaced.

The overall objective of the study referred to in this paper has been refining the current models of CVS with its nervous control (CVSNC) by improving the part of the model related to ventricle subsystem. In detail, that means:

- setting up a model at a physiological level of the CVS with its nervous control, having a medium degree of complexity.
- establishing a model of the cardiovascular system with its nervous control based on human characteristics;
- inserting models of the heart valves using an orifice model from fluid mechanics;
- testing the behavior of the model in closed-loop conditions in a normal scenario (healthy person).

Finally, the benefits of proposed modifications consist in the ability of the obtained model to capture more accurately dynamic behaviors specific to pathological scenarios like valve disease, myocardial infarction, hemorrhage etc.

The paper presents in the second chapter the structure of

978-1-4673-2529-5/12/$31.00 ©2012 IEEE

the CVSNC. Chapter 3 describes the mathematical model of the CVSNC. Chapter 4 details the behavior of the CVSNC model in a case study, relating its simulation results to reference data and to a basic model from [5]. Finally, conclusions are extracted and future research directions are provided.

II. Structure of the CVSNC

Regarding the model of CVSNC, two remarks are worth mentioning. First, the structure of CVCNC represents a conceptual model which implicitly exists in [5] (addressed here as the I-CVSNC), with differences in the presentation manner and level of detail. Consequently, the conceptual structures of the CVSNC and I-CVSNC are the same. Secondly, the differences between I-CVSNC and CVSNC consist in the mathematical models associated to different component subsystems.

The CVSNC structure is illustrated Fig. 1, and it simplifies the more complex one presented in [3], where additional nervous control loops were included in the representation. In the model, the retained nervous control loop is the baroreflex loop, and therefore only the baroreceptors placed in the Carotid Sinus are considered.

The functioning of the heart and vascular system are controlled by the medulla oblongata, which acts via the signals n_p and n_s like a two-output controller for the cardiovascular system. The control of the CVS is done based on the nervous signals coming from the baroreceptors (n_{br}) and from higher nervous centers (n_r). The medulla oblongata acts on the CVS thorough the peripheral autonomic nervous system (PANS), which is divided into the parasympathetic and sympathetic divisions, controlled by n_p respectively n_p. The parasympathetic subsystem acts only on the heart, slowing the heartbeat (n^p_{HR}), while the sympathetic subsystem acts on the heart accelerating the heartbeat (n^s_{HR}). Additionally, the sympathetic subsystem affects also the contractility of the heart (n^s_{CV}), the peripheral resistance of the arteries (n^s_R) and unstressed volume of the large veins (n^s_V).

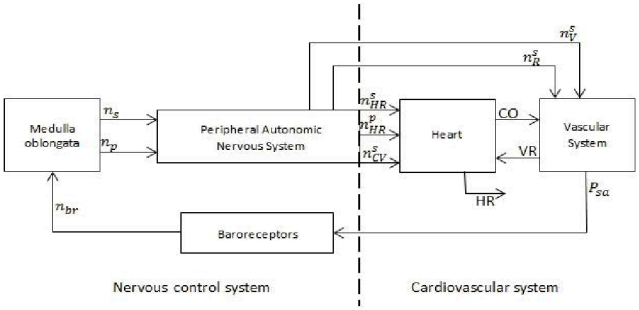

Fig. 1. Block diagram of the CVSNC and the main interaction signals.

A somehow detailed scheme of the Heart System is presented in Fig. 2. All the arrows corespond to signals. The double line arrows corespond to signal pairs shown in the figure. The preasure signals P_{pa} and P_{sa}, not shown in Fig. 1, are provided by the vascular system.

The Heart Systems is modeled by the interaction of three subsystems: the sino-atrial node (SAN), the Right Heart (RH) and the Left Heart (LH). The RH and LH are each formed out of corresponding atrium and ventricle. Here, F_{ra} means the input flow for the RH, F_{la} is the input flow for the LH, F_{or} is the output flow of the RH and F_{ol} is the output flow of the LH. The contraction process of the ventricles is influenced by: the SAN through the signal u, the sympathetic activity (n^s_{CV}) and the venous return (VR). The signal u has a saw tooth shape and dictates as well the contraction onset moment as the contraction evolution. This can be explained by the fact that the signal u has two time variable information carrier components, the heart period T, whose inverse is the heart rate HR (HR=1/T), and the instantaneous value u(t). It is also important to mention here that in this study the atrium contraction is neglected.

Figures 3 and 4 give an insight into RH, respectively LH. The first figure shows from an informational point of view the interactions at the level of the RH and the interactions of RH with upstream and downstream subsystems. The connection between the RA and the RV is done through the tricuspid valve (TV), and characterized by the pressures P_{ra} and P_{rv} and by the flow F_{tv}. The connection between the RV and pulmonary artery (PA) is done through the pulmonary valve (PV), and characterized by pressures $P_{max,rv}$ and P_{pa} and by the flow F_{or}. P_{pa} is the pressure from the PA, which, as mentioned before, does not appear in Fig. 1. Mutatis mutandis, the above considerations hold also for Fig. 4.

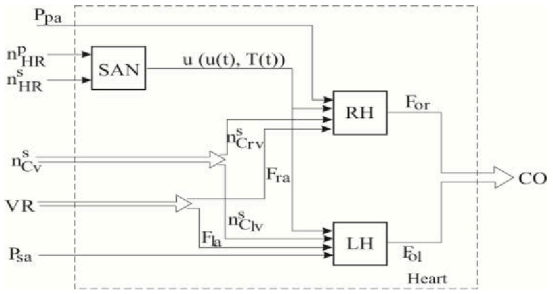

Fig. 2. The Heart System

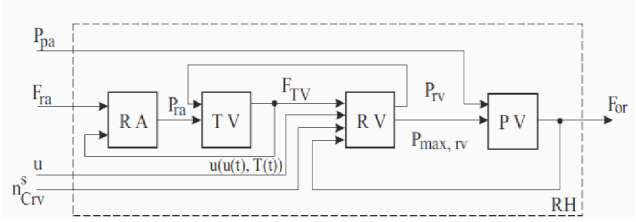

Fig. 3. The right heart system.

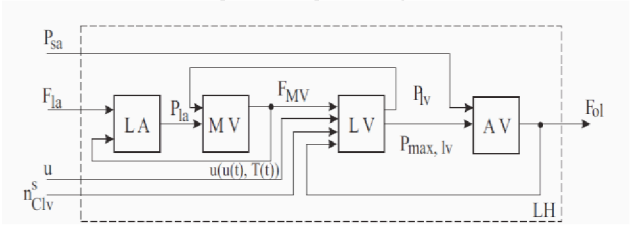

Fig. 4. The left heart system.

In respect with I-CVSNC (the model from [5]), in Fig. 3 and 4 some of the signal notations were changed: n^s_{Clv}/ n^s_{Crv} was used instead of $E_{max,lv}$/ $E_{max,rv}$. F_{MV}/F_{TV} was used instead of $F_{i,l}$/$F_{i,r}$, F_{la}/F_{ra} refer to the venous return, and E_V was used instead of φ.

III. Mathematical Model of the CVSNC

In the followings, the conceptual model presented in the previous chapter is used to introduce the I-CVSNC model, to describe the adjustments that lead to the CVSNC, regarding different subsystems models and parameters. The aim of proposed adjustments was to improve the I-CVSNC model in order to capture the functionality of CVS as close as possible to the real situation.

In respect to the I-CVSNC model, used as reference, two main adjustments will be done.

i) For describing the process of ventricle contraction in [5], an activation function *φ(t)* based on animal experimental data, is used. Subsequently, this function was replaced in literature by an elastance function E_V, based on human experimental data ([6]). The elastance function – or simply referred as elastance – describes a parametrical control mode carried out by the nervous system over the ventricles. This context justifies the use of the elastance from [6] in the I-CVSNC, which is considered to be a more elaborated model ([5]).

ii) The models from [5] and [6], as well as other subsequent models from the literature, were developed considering in a first approximation that the flow through valves can be described as a laminar flow process through a rigid pipeline characterized by a certain hydraulic resistance (R). As it is pointed out in [7], the flow processes are actually inertial orifice flow processes, i.e. the valves have a certain dynamics – which means that they do not open and close instantaneously. Consequently, the I-CVSNC model should be adjusted also form this point of view. As result, it is of interest to import the valve models from [7] in the I-CVSNC model.

The part of I-CVSNC model which embeds the left ventricle compartment, together with the valves (in accordance with Fig. 4 this means MV+LV+AV), is described thorough equations (1)-(6), which were written based on the observation at the end of Section II. This subsystem is from a dynamical point of view a first order nonlinear time-varying system. The state equation and the two output equations are:

$$\frac{dV_{lv}(t)}{dt} = F_{MV}(t) - F_{ol}(t) \tag{1}$$

respectively

$$\begin{aligned} P_{\max,lv}(t) &= E_V(t)\cdot n^s_{Clv}(t)\cdot\left(V_{lv}(t) - V_{u,lv}\right) + \\ &+ \left(1 - E_V(t)\right)\cdot P_{0,lv}\cdot\left(e^{k_{E,lv}V_{lv}(t)} - 1\right), \quad 0 \le E_V(t) \le 1 \end{aligned} \tag{2}$$

$$P_{lv}(t) = P_{\max,lv}(t) - R_{lv}(t)\cdot F_{ol}(t) \tag{3}$$

The flows from (1) and the activating function (elastance) from (2) are given by the non-inertial dependencies:

$$F_{MV}(t) = \begin{cases} 0 & ,P_{la}(t) \le P_{lv}(t) \\ \dfrac{P_{la}(t) - P_{lv}(t)}{R_{la}} & ,P_{la}(t) > P_{lv}(t) \end{cases}, \tag{4}$$

$$F_{ol}(t) = \begin{cases} 0 & ,P_{\max,lv}(t) \le P_{sa}(t) \\ \dfrac{P_{\max,lv}(t) - P_{sa}(t)}{R_{lv}(t)} & ,P_{\max,lv}(t) > P_{sa}(t) \end{cases}, \tag{5}$$

respectively

$$E_V(t) = \begin{cases} \sin^2\left[\dfrac{\pi\cdot T(t)}{T_{sys}(t)}\cdot u(t)\right] & ,0 \le u(t) \le \dfrac{T_{sys}(t)}{T(t)} \\ 0 & ,\dfrac{T_{sys}(t)}{T(t)} \le u(t) \le 1 \end{cases}. \tag{6}$$

where $T_{sys}(t) = T_{sys,0} - k_{sys}\cdot\dfrac{1}{T(t)}$.

The CVSNC keeps the state and output equations of the I-CVSNC, using instead of equations (4) and (5), corresponding to observation ii), the following models:

$$F_{MV}(t) = K_{v,MV}\cdot AR_{MV}(t)\cdot\mathrm{sgn}\left(P_{la}(t) - P_{lv}(t)\right)\sqrt{\left|P_{la}(t) - P_{lv}(t)\right|} \tag{7}$$

$$F_{ol}(t) = K_{v,ol}\cdot AR_{ol}(t)\cdot\mathrm{sgn}\left(P_{\max,lv}(t) - P_{sa}(t)\right)\sqrt{\left|P_{\max,lv}(t) - P_{sa}(t)\right|} \tag{8}$$

where

$$AR_{MV}(t) = \frac{\left(1 - \cos(sat(\theta_{MV}(t)))\right)^2}{\left(1 - \cos(\theta_{MV,\max})\right)}, AR_{ol}(t) = \frac{\left(1 - \cos(sat(\theta_{ol}(t)))\right)^2}{\left(1 - \cos(\theta_{ol,\max})\right)}. \tag{9}$$

$$\frac{d^2\theta_{MV}(t)}{dt^2} = K_{p,MV}\cdot\left(P_{la}(t) - P_{lv}(t)\right)\cdot\cos(\theta_{MV}(t)) - K_{f,ol}\cdot\frac{d\theta_{MV}(t)}{dt}$$

$$\frac{d^2\theta_{ol}(t)}{dt^2} = K_{p,ol}\cdot\left(P_{lv}(t) - P_{sa}(t)\right)\cdot\cos(\theta_{ol}(t)) - K_{f,ol}\cdot\frac{d\theta_{ol}(t)}{dt}$$

$$sat(x) = \begin{cases} 0, x < 0 \\ x, 0 < x < \theta_{\max} \\ \theta_{\max}, x > \theta_{\max} \end{cases} \tag{10}$$

Also, for the elastance from (6), according to the observation i), there is

$$E_V(t) = \begin{cases} \dfrac{E_d}{n^s_{Cv}(t)} + \dfrac{n^s_{Cv}(t) - E_d}{2n^s_{Cv}(t)}\left[1 - \cos\left(\pi\cdot\dfrac{u(t)}{T_{sys}(t)}\right)\right] & ,0 \le u(t) \le \dfrac{T_{sys}(t)}{T(t)} \\ \dfrac{E_d}{n^s_{Cv}(t)} + \dfrac{n^s_{Cv}(t) - E_d}{2n^s_{Cv}(t)}\left[1 + \cos\left(2\pi\cdot\dfrac{u(t)}{T_{sys}(t)}\right)\right], & \dfrac{T_{sys}(t)}{T(t)} \le u(t) \le \dfrac{3}{2}\cdot\dfrac{T_{sys}(t)}{T(t)} \\ \dfrac{E_d}{n^s_{Cv}(t)} & ,\dfrac{3}{2}\cdot\dfrac{T_{sys}(t)}{T(t)} \le u(t) \le 1 \end{cases} \tag{11}$$

where $T_{sys}(t) = T_{sys,0} - k_{sys}\cdot\dfrac{1}{T(t)}$ (12).

It should be observed that by replacing the expression of $E_V(t)$ from (11) in (2), $n^s_{Cv}(t)$ (which takes the values n^s_{Clv}/ n^s_{Crv}) is simplified, so the expressions finally used are $E_V(t)n^s_{Cv}(t) = E_d + \left(n^s_{Cv}(t) - E_d\right)\left(1 - \cos(\pi u(t)/T_{sys}(t))\right)$ etc.

In the simulations from the current research, the authors adopted an alternative simplified solution, considering in (11) that $n^s_{Cv}(t) = E_{es}$, where E_{es} is the nominal value of the maximum elastance, taken from [6]. The approximation was shown to be feasible in the simulations from the next section.

The following details are necessary for a complete understanding of the CVSNC model described by equations (1)-(3) and (7)-(12):

- In (2), $V_{u,lv}$ is the unstressed volume, while $P_{0,lv}$ and $k_{E,lv}$ are constant dimensional parameters.
- In (3), R_{lv} was expressed like in [5] as $k_{R,lv} \cdot P_{max,lv}$, with $k_{R,lv}$ a constant dimensional parameter.
- The square root functions from (7) and (8) are characteristic for flows through orifice ([8]); the formulas from (7) and (8) correct those from [7] by considering a possibility of sign change, and so negative flow existence.
- The AR terms from (7) and (8) represent normalized valve opening areas.
- In (9), θ represents the angle for the valve leaflet positions, and based on (10) it varies between θ=0 (fully closed) and θ= θ_{max} (fully open).
- The sat function from (9), expressed in (10), was introduced after observing that formulas from [7] which do not contain the saturation function allow a non-physiological variation of θ.
- In (10), K_p and K_f are constant dimensional parameters.
- Equations (10) introduce a dynamic component in the valve opening and closing which makes possible for negative flow to appear.
- E_d, the diastolic elastance from (11), is constant parameter.
- For the systole time interval T_{sys} equations (12) from the I-CVSNC was used, although in [6] a different expression was proposed. The reason for doing this was that by using the formula from [6] $K \cdot \sqrt{T}$ no significant changes were observed during simulations, and we intended to make as few modifications as possible in the I-CVSNC.

Equations, similar to those above, were used for the right heart.

IV. CVSNC Behavior – A Case Study

The chapter focuses on comparing the results from CVSNC model with experimental data from the literature. The first section describes the parameters of the CVSNC model. Further, reference data is extracted from the literature and it is set beside the data taken over from the CVSNC model simulations. Finally, the CVSNC–I-CVSNC relation is analyzed, different signal evolutions are compared and conclusions are formulated.

A. CVSNC model parameters

The section provides the values of the parameters used by the CVSNC model. Thus, for the left and right heart, the parameters were taken from [5] and they are shown in Table 1. The parameters describing the heart beat, $T_{sys,0}$=0.5 s, and k_{sys}=0.075 s^2, were also taken from [5].

TABLE 1
Parameters describing the left and right heart

Left Heart	Right Heart
$V_{u,lv}$=16.77 ml	$V_{u,rv}$=40,8 ml
$E_{max,lv}$=2.95 mmHg/ml	$E_{max,rv}$=1.75 mmHg/ml
$k_{E,lv}$=0.014 ml^{-1}	$k_{E,rv}$=0.011 ml^{-1}
$P_{0,lv}$=1.5 mmHg	$P_{0,rv}$=1.5 mmHg
R_{la}=2.5 e-3 mmHg s ml^{-1}	R_{ra}=2.5e-3 mmHg s ml^{-1}

The values for E^{lv}_{es}, E^{lv}_{d}, E^{rv}_{es} and E^{rv}_{d} used in (11) were adopted, as in Table 2, from [6], where a deeper analysis was done regarding these parameters.

TABLE 2
Parameters describing the left and the right heart

Left Heart	Right Heart
E^{lv}_{d} = 0.13 mmHg/ml	$E^{rv}_{d} = 0.07\ mmHg/ml$
$E^{lv}_{es} = 2.6\ mmHg/ml$	$E^{rv}_{es} = 1.4\ mmHg/ml$

When introducing equation (10) in the current model, in order to obtain an appropriate behavior (waveform) of blood flow and pressure some adjustments needed to be done. The first mandatory step was to adjust the equations taken from [7]. The main issue in order to integrate the representation of the valves from [7] was to obtain proper values for the parameters because the data in a raw form entailed no satisfactory results (the resulted waveform did not fit within the limits considered satisfactory).

To adjust the parameters of the CVSNC model when introducing equations (7)-(10) associated to representations of the heart valves, all their values were quasi-empirically calibrated regarding to desired simulation results. After a first study, the $K_{v,i}$ (where "i" corresponds to ol, MV, or and TV) constants revealed to be the most influential. Values of parameters $K_{p,i}$ and $K_{f,i}$ were also calibrated, but their influence over the analyzed signals was less significant. Table 3 presents final values for $K_{v,i}$, $K_{p,i}$, $K_{f,i}$.

TABLE 3
Parameters describing the valve opening model in the left and right heart

Systemic Part	Pulmonary Part
$K_{v,ol} = 78\ ml/(s \cdot mmHg^{0.5})$	$K_{v,or} = 85\ ml/(s \cdot mmHg^{0.5})$
$K_{v,MV} = 110\ ml/(s \cdot mmHg^{0.5})$	$K_{v,TV} = 200\ ml/(s \cdot mmHg^{0.5})$
$K_{p,ol} = 27500\ ml/(s^2\ mmHg)$	$K_{p,or} = 50000\ ml/(s^2\ mmHg)$
$K_{f,ol} = 250\ s^{-1}$	$K_{f,or} = 500 s^{-1}$
$K_{p,MV} = 27500\ ml/(s^2\ mmHg)$	$K_{p,TV} = 27500\ ml/(s^2\ mmHg)$
$K_{f,MV} = 250\ s^{-1}$	$K_{f,TV} = 250\ s^{-1}$

B. Reference data

This section points out the experimental data that will be used in assessing the simulation results. The waveforms, considered being representative for the processes of CVS, will be highlighted for qualitative validations, while some measurable indicators (markers) will be defined for quantitative validations.

Because the aim of the current study is to improve the part of the model related to ventricle subsystem, the signals related to the two ventricle compartments will be of main interest. Because each of the two ventricle subsystems is interconnected with an up-stream subsystem and a down-stream subsystem, the dynamics of these subsystems should also be taken into account. The improved model of each such connections is obtained assuming that the subsystems are separable (this means that the interconnection does not affect the model of any part of the connection).

Thus, for the Atrium up-stream subsystems the signals P_{la}/P_{ra} and F_{la}/F_{ra} are of interest. Subsequently, for the Arteries down-stream subsystems the signals P_{sa}/P_{pa} are of interest. All these will be considered for a nominal heart rate (HR) of 60 bpm. Due to sparse information on RV waveforms available in the literature, wherever possible these waveforms will be considered to be similar to corresponding LV waveforms (RV waveforms will be considered to be a scaled version of LV waveforms).

For the P_{lv} and P_{rv} signals, the waveform from [9] was considered as reference (Fig. 6). The indicators defined for these signals are as follows:

- *maximum ventricle pressure* $P_{i,max}$: $P_{lv,max}$=120 mmHg, $P_{rv,max}$=30mmHg (based on values from Wiggers diagrams);
- *maximum slope of ventricle pressure* $(dP_i/dt)_{max}$: $(dP_{lv}/dt)_{max}$=1146 mmHg/s, $(dP_{rv}/dt)_{max}$=369 mmHg/s (based on [10], [11], [12], scaled according to $P_{i,max}$ ratio);
- *minimum slope of ventricle pressure* $(dP_i/dt)_{min}$: $(dP_{lv}/dt)_{min}$ = -1060 mmHg/s, $(dP_{rv}/dt)_{min}$ = -396 mmHg/s (based on values from [10], [11] and [12]).

For V_{lv} and V_{rv} signals the waveform from [9] were considered as reference (Fig. 7). For assessing the correlation between ventricle pressure and ventricle volume, the pressure volume characteristic from [13] is also considered (Fig. 8). In this case the associated indicator is:

- *maximum ventricle volume (end diastolic volume)* $V_{i,max}$: $V_{lv,max}$=150 ml, $V_{rv,max}$=173 ml (based on [14]).

For the F_{ol} and F_{or} signals the waveform from [9] was considered as reference (Fig. 9). The corresponding indicators are:

- *maximum ventricle output flow*: $F_{ol,max}$=500 ml/s, $F_{or,max}$=434.25 ml/s (based on values from [9] and [12], scaled according to the $P_{rv,max}$ ratio);
- *duration of ejection (non zero flow)* $T_{i,Q}$: $T_{LV,Q}$= 0.18 s, $T_{RV,Q}$= 0.2 s (based on values from [9] and [15], scaled according to the nominal HR).

Due to spare data found in literature on humans for F_{la} and F_{ra} signals, their waveforms is considered somehow similar to the waveform of F_{ol}. A single indicator is defined:

- *maximum atrial output flow*: $F_{la,max}$=340 ml/s, $F_{ra,max}$=240 ml/s (based on values from [16] and [17]).

The signals P_{sa} and P_{pa} have as reference waveform that from Fig. 6 (dashed lines). As indicators, there are:

- *maximum arterial pressure*: $P_{sa,max}$=120 mmHg, $P_{pa,max}$= 30 mmHg (based on values from [18]);
- *minimum arterial pressure*: $P_{sa,min}$= 80 mmHg, $P_{pa,min}$= 10 mmHg (based on values from [18]).

Due to the low levels of pressures P_{la} and P_{ra} very few measurements can be found in the literature. Moreover, the influence of these signals variations over the CVS is of marginal importance. However, the study includes these signals through the waveform $P_{la}(t)$ from Fig. 6. The maximum level indicator is:

- *maximum atrium pressure* $P_{ia,max}$: $P_{la,max}$=10 mmHg, $P_{ra,max}$= 5 mmHg (based on values from [18])

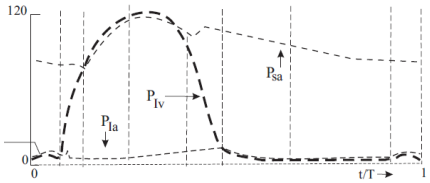

Fig. 6 P_{lv} [mmHg] signal used as reference

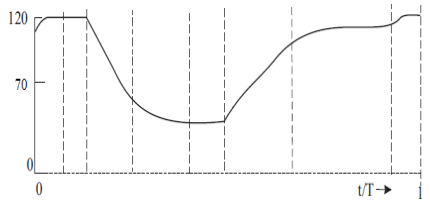

Fig. 7 V_{lv} [ml] signal used as reference

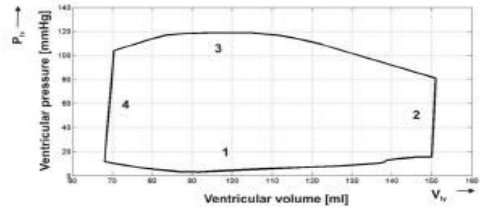

Fig. 8 Pressure-volume relations for the LV

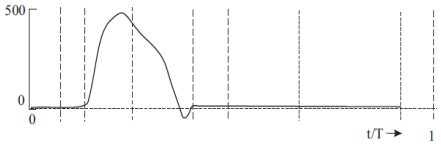

Fig. 9 F_{ol} signal used as reference

C. Baseline simulation

As it was pointed out previously the parameters values were assigned with the goal of representing the CVS of healthy human subject. The cardiovascular variables were extracted in a beat-to-beat manner from the model.

In section IV.B the chosen reference data from the literature was illustrated. The presented data is summarized in the left column of Table 4 and compared with the simulation data (right column of the table) obtained through the CVSNC model. Simulation results are presented in detail in the next section (IV.D).

As in can be noticed from Table 4 the model is capable to reproduce adequately the behavior of the cardiovascular system with its nervous control in a normal scenario. Here, 'normal scenario' refers to the population against which the model response is compared, and it means a scenario that addresses the CVS behavior in a steady state regime in which the body is unstressed. Note that it is a periodic steady state, i.e. a regime in which each variable is a periodically function of the time. In this sense, the model

framework can be considered a valid representation of the cardiovascular system developed for healthy population.

TABLE 4
Left Heart and Right Heart signal analysis

REFERENCE VALUES	CVSNC MODEL VALUES
$P_{lv,max}$=120 mmHg	$P_{lv,max}$=115 mmHg
$dP_{lv,max}/dt$=1146 mmHg/s	$dP_{lv,max}/dt$=1000 mmHg/s
$dP_{lv,min}/dt$= -1060 mmHg/s	$dP_{lv,min}/dt$ = -727 mmHg/s
$V_{lv,max}$= 150 ml	$V_{lv,max}$= 90 ml
$F_{ol,max}$=500 ml/s	$F_{ol,max}$=350 ml/s
$T_{LV,Q}$= 0.18 s	$T_{LV,Q}$= 0.18 s
$F_{la,max}$=340 ml/s	$F_{la,max}$=320 ml/s
$P_{la,max}$=10 mmHg	$P_{la,max}$=15 mmHg
$P_{rv,max}$= 30 mmHg	$P_{rv,max}$= 32 mmHg
$dP_{rv,max}/dt$= 369 mmHg/s	$dP_{rv,max}/dt$= 400 mmHg/s
$dP_{rv,min}/dt$= -396 mmHg/s	$dP_{rv,min}/dt$= -400 mmHg/s
$V_{rv,max}$= 173 ml	$V_{rv,max}$= 125 ml
$F_{or,max}$= 434.25 ml/s	$F_{or,max}$= 300 ml/s
$T_{RV,Q}$= 0.2 s	$T_{RV,Q}$= 0.34 s
$F_{ra,max}$= 240 ml/s	$F_{ra,max}$= 220 ml/s
$P_{ra,max}$= 5 mmHg	$P_{ra,max}$= 9 mmHg

D. CVSNC and I-CVSNC comparison

The section analyzes the simulation results obtained using the CVSNC model, respectively the I-CVSNC model. The characteristics of the waveforms are analyzed especially in the parts where modifications were carried out.

Fig. 10 shows the waveform for the elastance (E_V) obtained with equation (6). Note that the maximal value of E_V for I-CVSNC is 1, because it actually denotes a normalized component of the elastance (the amplitude would be given by the maximum elastance $n^s_{C_V}(t)$), and it is the same E_V for both ventricles. Fig. 11 shows the waveform of E_V obtained with equation (11), in the CVSNC model. As it can be observed, an elastance is associated for each ventricle in the CVSNC model. Also, the maximal value of E_V for RV is 1.5 and for the LV is 2.5.

Fig. 12 shows the right and left ventricle pressures (P_{rv} and P_{lv}) obtained with equation (3). It can be observed that the signals upper limit is 35 mmHg for RV, and 150 mmHg for LV. Fig. 13 illustrates the waveforms obtained with the CVSNC model. The maximal value for the pressure in RV in this situation is 35 mmHg, and in LV is 120 mmHg.

Fig. 14 shows the blood flow entering in right and left ventricles (F_{MV} and F_{TV}) obtained with equation (4) in the I-CVSNC. The maximal value of F_{MV} is 1000 ml/s, and of F_{TV} is 1700 ml/s. Fig. 15 shows F_{MV} and F_{TV} in the CVSNC model where the mitral and tricuspid valve were modeled with equation (7). A major difference can be noticed between the two models. The maximal values in this situation are 130 ml/s provided by the TV, respectively 350 ml/s provided by the MV.

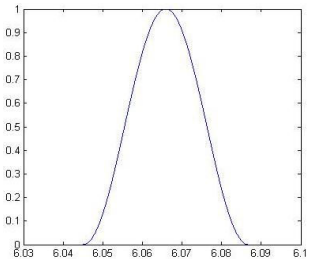
Fig. 10 Elastance waveform $E_V(t)$ for LV and RV from I-CVSNC

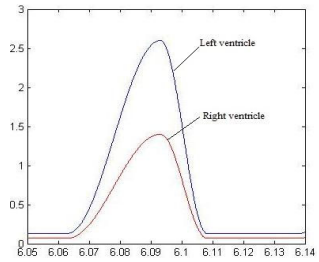

Fig. 11 Elastance waveform $E_V(t)$ for LV and RV from CVSNC

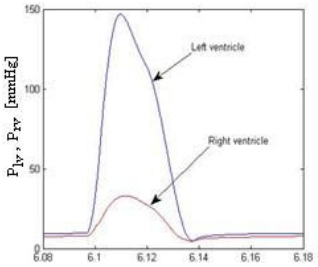

Fig. 12 $P_{rv}(t)$, $P_{lv}(t)$ - I-CVSNC

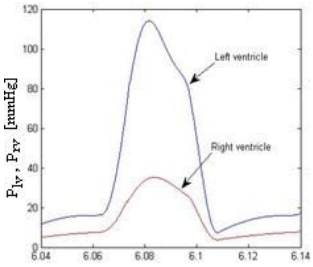

Fig. 13 $P_{rv}(t)$, $P_{lv}(t)$ – CVSNC

Fig. 16 presents the cardiac output for right and left ventricles (F_{or} and F_{ol}) obtained with equation (5) in the I-CVSNC model. The maximal value for F_{or} is 650 ml/s, and for F_{ol} is 900 ml/s. Fig. 17 presents the outputs of the aortic and pulmonary aortic valve obtained with equation (8), in the CVSNC model. The maximal value for F_{or} is 300 ml/s, and for F_{ol} is 350 ml/s.

Figures 18 and 19 show the volume for RV and LV (V_{rv} and V_{lv}) obtained with I-CVSNC model, respectively with CVSNC model. In the first situation maximal value for V_{rv} is 170 ml, and for V_{lv} is 140 ml. With the CVSNC model, the maximal value for V_{rv} is 125 ml and for V_{lv} is 95 ml.

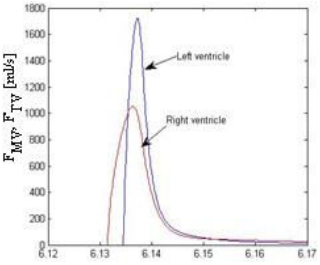

Fig. 14 $F_{MV}(t)$, $F_{TV}(t)$ - I-CVSNC

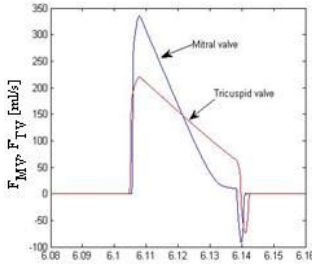

Fig. 15 $F_{MV}(t)$, $F_{TV}(t)$ - CVSNC

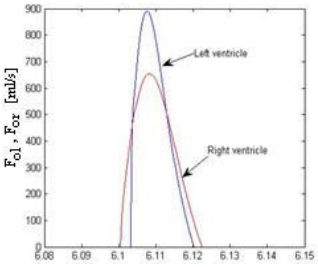

Fig. 16 $F_{or}(t)$, $F_{ol}(t)$ - I-CVSNC

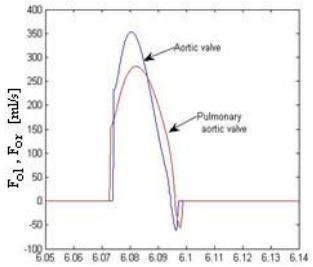

Fig. 17 $F_{or}(t)$, $F_{ol}(t)$ - CVSNC

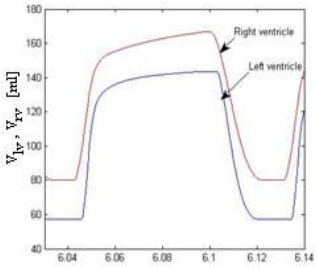

Fig. 18 $V_{rv}(t)$, $V_{lv}(t)$ - I-CVSNC

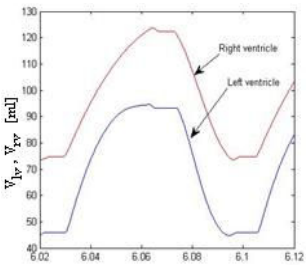

Fig. 19 $V_{rv}(t)$, $V_{lv}(t)$ - CVSNC

V. CONCLUSIONS

In the current paper a model was established to simulate more accurately the human CVS and the corresponding nervous control (the CVSNC model). After setting up the starting point as the I-CVSNC model, developed in [5], the first step was to improve the elastance function of the ventricle with one that was defined following human characteristics. Afterwards, the valve models were improved, setting up an inertial type model that is much closer to reality. A parameter correlation and calibration procedure was necessary to finalize and refine the model.

The behavior of the CVSNC model was analyzed in a normal scenario through simulations, i.e. a steady state scenario in which the body is unstressed. The simulations reveal significant differences between the initial model (I-CVSNC) and the proposed improved model (CVSNC) in favor of the latter. It is expected that the improvements proposed in the current study will prove to play a more important role in representing pathological scenarios like valve disease, myocardial infarction, or hemorrhage. Consequently, as future work, the model will be tested in a more elaborate manner in several pathological scenarios, and will be further validated based on experimental data.

REFERENCES

[1] D. Deserranno, M. Kassemi, J. D. Thomas, "Incorporation of myofilament activation into a lumped model of the human heart", *Annals of Biomedical Engineering*, 34 (3), pp. 321-336, 2007.

[2] B.W. Smith, J.G. Chase, R.I. Nokes, G.M. Shaw, G. Wake, "Minimal haeomdyanmic system model including ventricular interaction and valve dynamics", *Medical Engineering & Physics*, Vol. 26, pp. 131-139, 2004.

[3] A. Codrean, A. Korodi, T.-L. Dragomir, L. Kovács, "Up to date issues on modeling the nervous control of the cardiovascular system on short-term," Proc. of 18th IFAC World Congress, 2011.

[4] A. Codrean, "Modeling physiological control mechanisms", Bachelor Thesis, "Politehnica" University of Timisioara, 2010.

[5] M. Ursino, "Interaction between carotid baroregulation and the pulsating heart: a mathematical model", *Am. J. Physiol. Heart Circ. Physiol* 275: H1733- H1747, 1998.

[6] T. Heldt, "Computational models of cardiovascular response to orthostatic stress", Ph.D. Thesis, MIT, 2004.

[7] T. Korakianitis, Y. Shi, "A concentrated parameter model for the human cardiovascular system including heart valve dynamics and atrioventricular interaction", *Med. Eng. Phys.* 28(7):613-628, 2006

[8] M. Jelali, A. Kroll, Hydraulic servo-systems, Advances in Industrial Control Springer Series, Ch. 3 Physical Fundamentals of Hydraulics, pp. 29-52, 2002.

[9] A. Despopoulos, S. Silbernagl, *Color Atlas of Phys.*, 5th Ed., 2003.

[10] Y. L. Zhong, R. S. Tan, D. N. Ghista, E. Yin-Kwee Ng, L. P. Chua and G. S. Kassab, "Validation of a novel noninvasive cardiac index of left ventricular contractility in patients", *Am J Physiol Heart Circ Physiol*, Vol 292, pp. 2764-2772, 2007.

[11] M. R. Starling, "Effects of low-dose flosequinan on leftventricular systolic and diastolic chamberperformance", *American Heart Journal*, Vol. 128, No. 1, pp. 124-133, 1994.

[12] M. Karamanoglu, M. McGoon, R. P. Frantz, R. L. Benza, R. C. Bourge, R. J. Barst, B. Kjellstrom, T. D. Bennett, "Right ventricular pressure waveform and wave reflection analysis in patients with pulmonary arterial hypertension", *Chest*, Vol.132, pp. 37-43, 2007.

[13] R. M. Berne, M. N. Levy, *Physiology*, C. V. Mosby, 2003.

[14] L. E. Hudsmith, S. E. Petersen, J. M. Francis, M. D. Robson, S. Neubauer, "Normal human left and right ventricular and left atrialdimensions using steady state free precession magneticresonance imaging", *Journal of Cardiovascular Magnetic Resonance*, Vol. 7, pp.775–782, 2005.

[15] A. Lopez-Candales, K. Edelman, B. Gulyasy, M. D. Candales, "Differences in the duration of total ejection between right and left ventricles in chronic pulmonary hypertension", *Echocardiography*, Vol. 28, Is. 5, pp. 509-515, 2011.

[16] J.R.T.C.Roelandt, M.Pozzoli, "Non-invasive assessment of left ventricular diastolic (Dys) function and filling pressure", *Thoraxcenter J.*, Vol 13, No. 2, 2001.

[17] P. Couture, A. Y. Denault, P. Sheridan, S. Williams, R. Cartier, "Partial inferior vena cava snaring to controlischemic left ventricular dysfunction", *CAN J ANESTH*, Vol. 50, No. 4, pp. 404–410, 2003.

[18] W. F. Boron, E. L.Boulpaep, "Medical physiology: a cellular and molecular approach", Saunders/Elsevier, 2009.

[19] M. Olufsen, J. Ottesen, H. Tran, L. Lipsitz, and V. Nivak, "Modeling baroreflex regulation of the heart rate during orthostatic stress," Am. J. Physiol. Reg. Integr. Comp. Physiol., Vol. 291, pp. 1355-1368, 2006.

[20] V. Le Rolle, A.I. Hernandez, P.Y. Richard, and G. Carrault, "An autonomic Nervous System Model Applied to the Analysis of Orthostatic Stress," Modelling and Simulation in Engineering, Vol. 2008, Article ID 427926.

[21] K. Lu, J.W.Jr. Clark, F.H. Ghorbel, D.L. Ware, A. Bidani, "A human cardiopulmonary system model applied to the analysis of the valsava maneuver," Am. J. Physiol. Heart. Circ. Physiol., Vol. 281, pp. 2661-2679, 2001.

[22] L.M. Ellewin, "Cardiovascular and Respiratory Regulation, Modeling and Parameter Estimation," PhD. Thesis, North Carolina State University, 2008.

[23] J.J. Batzel, F. Kappel, D. Schneditz, H. T. Tran, Cardiovascular and Respiratory Systems, SIAM, Philadelphia, 2007.